Design, Synthesis, and Properties of Asymmetrical Heteroacene and Its Application in Organic Electronics

Chunyan Du,[†,‡] Yunlong Guo,[†,‡] Jianming Chen,[†,‡] Hongtao Liu,[†,‡] Ying Liu,[†,‡] Shanghui Ye,[†,‡] Kun Lu,[†,‡] Jian Zheng,[†,‡] Ti Wu,[†,‡] Yunqi Liu,*[,†] Zhigang Shuai,[†] and Gui Yu[†]

Beijing National Laboratory for Molecular Sciences, Key Laboratory of Organic Solids, Institute of Chemistry, Chinese Academy of Sciences and Graduate School of Chinese Academy of Sciences, Beijing 100190, China

Received: February 5, 2010; Revised Manuscript Received: May 10, 2010

Asymmetrical heteroacene up to six fused rings, tetraceno[2,3-*b*]benzo[*d*]thiophene (TBT), was synthesized facilely and its physicochemical properties and device applications were investigated. Field-effect transistors (FETs) fabricated with TBT as semiconducting layers showed carrier mobility up to 0.13 $cm^2\ V^{-1}\ s^{-1}$. The transistors also exhibited a photoeffect and a ratio of photocurrent to dark-current as high as 10^4 was achieved. Density functional theory and FET results demonstrated that, for bent heteroacenes, increasing a benzene ring in conjugation length would not result in higher field-effect mobility, and the FET performance is more influenced by the thin film morphology. All these results suggest that the introduction of heteroatoms provides an efficient route for exploring the chemistry of larger acenes.

Introduction

Organic semiconductors have attracted much attention in recent years because of their potential applications in electronics, photonics, and optoelectronics.[1] In contrast to conjugated polymers, conjugated oligomers are characterized by their well-defined structures and superior chemical purity.[2] Among them, acenes, which are composed of linearly annelated benzene rings, have been the focus of research interest because of their enhanced degree of π-conjugation, highly efficient photoluminescence, and remarkable charge mobility.[3] Tetracene[4] and pentacene,[5] two examples of acenes, have been utilized extensively in organic electronics; higher acenes, however, remain virtually unknown because they are very easily photooxidized.[6] Recently, Neckers reported the synthesis of hexacene and heptacene embedded in rigid polymeric media via photochemical route; however, these molecules only show lifetimes of about 12 and 4 h.[7]

Many efforts have been devoted to improve the resistance of acenes to photooxidation. Anthony's group reported the synthesis and characterization of silylethynylation hexacene and heptacene derivatives.[8] However, the triisopropylsilyl ethynyl (TIPS) group seems not to be sufficiently bulky to prevent Diels−Alder addition of the alkynes across reactive acenes, as neither the TIPS-substituted hexacene nor the heptacene was stable in solution or in the solid state. Thus, the author chose the bulkier tri-*tert*-butylsilyl acetylene group, leading to a moderate increase in the stability of these derivatives. Wudl's group synthesized functionalized heptacene with the phenyl group and the alkylsilylethynyl group substituents and found a single crystal of the compound sufficiently stable for over 21 days.[9] More recently, Miller's group reported another stable heptacene derivative and demonstrated that not only alkylsilylethynyl groups but a combination of arylthio and *o*-dialkylphenyl substituents can be utilized to produce a persistent heptacene derivative.[10] The bulky substituent groups, however, may have disturbed the solid state stacking of these derivatives, and no field effect characteristics have been reported.

The higher oxidation potential and larger energy gap between the highest occupied molecular orbital (HOMO) and the lowest unoccupied molecular orbital (LUMO) of the aromatic ring of the heteroacenes vs the carbocyclic acenes make the former class of compounds ideal candidates for exploring the chemistry of larger acenes. Pentaceno[2,3-*b*]thiophene (PTT), which is pentacene fused with a terminal thiophene ring, was synthesized as a hexacene-like molecule.[11] Compound PTT was stored in a nitrogen glove box as it was still not stable under ambient conditions. Higher thienoacenes containing six to eight fused thiophene units have been synthesized, and these fused ring compounds not only retained the linear fused architecture of acenes but also showed improved stability under ambient conditions.[12] However, these thienoacenes are not as conjugated as their carbocyclic analogues and there are no reports yet about FET characteristics for these thienoacenes. It seems to be difficult to balance the conjugation and stability of heteroacenes. Therefore, it is urgent to probe the structure−property relationships of organic semiconductors, especially heteroacenes.

Previously, we reported the synthesis and field effect characteristics of the pentacene-like compound anthra[2,3-*b*]benzo[*d*]thiophene (ABT),[13] the compound ABT with introduction of a sulfur atom compared with pentacene exhibited better stability than pentacene and comparable FET performance. Expanding our study, we wondered if tetraceno[2,3-*b*]benzo[*d*]thiophene (TBT), in which one more benzene ring was fused with ABT, is a promising organic semiconductor. On the basis of the ring system, TBT is expected to have a longer, plate-like molecular shape and larger conjugation than ABT. Also, with the introduction of heteroatom, TBT is expected to afford a balance between the stability and conjugation of heterohexacene. Furthermore, TBT is expected to interact efficiently through intermolecular S···S or S···π contacts which can provide an alternative charge transport pathway other than $\pi-\pi$ interactions. Here, we report the synthesis, physicochemical properties of TBT, and its application in phototransistor

* To whom correspondence should be addressed. Phone: +86-10-62613253. E-mail: liuyq@iccas.ac.cn.
† Institute of Chemistry, CAS.
‡ Graduate School, CAS.

10.1021/jp101135e
Published on Web 05/18/2010

SCHEME 1: (a) Synthesis Route of compound TBT and (b) the Structure of Anthra[2,3-*b*]benzo[*d*]thiophene (ABT)

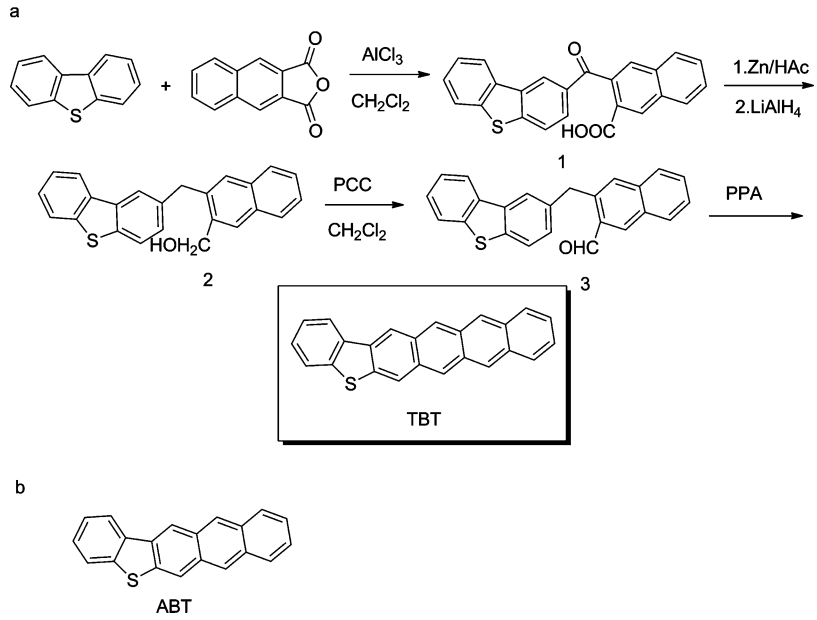

devices. A mobility up to 0.13 $cm^2\ V^{-1}\ s^{-1}$ has been achieved. Furthermore, the devices based on TBT exhibited a photoeffect and a ratio of photocurrent and dark-current (I_{ph}/I_{dark}, P) as high as 10^4 was achieved. We also gained some insight into the structure−property relationships of bent heteroacenes based on the experimental results and theory calculations. To the best of our knowledge, this is the first report of the study of phototransistor application and structure−property relationships based on heterohexacene. Our study made a good complement for the family of hexacene analogues.

Results and Discussion

Synthesis and Characterization. The synthesis of TBT was performed in four steps starting from commercially available dibenzothiophene as shown in Scheme 1. Friedel−Crafts reaction between dibenzothiophene and naphtho[2,3-*c*]furan-1,3-dione gave **1** in 84% yield. After two successive reduction steps on **1**, we obtained 3-(dibenzothiophene-2-ylmethyl)-naphthalen-2-ylmethanol (**2**). The methanol derivative **2** was oxidized with pyridinium chlorochromate to give 3-(dibenzothiophene-2-ylmethyl)-2-naphthaldehyde (**3**). The final product TBT was obtained by cyclization of naphthaldehyde derivative **3** in polyphosphoric acid (PPA) solution. Pure compound TBT was isolated by multitimes recrystallization in toluene and three-zone furnace sublimation as a purple powder. Its chemical structure was determined by EI-MS, ^{1}H NMR, and elemental analysis. The thermal property of TBT was evaluated by thermogravimetric analysis (TGA). The onset temperature of 339 °C was observed in TGA, demonstrating good thermal stability of TBT.

Electrochemical and Optical Properties. To obtain the HOMO level of compound TBT, we performed cyclic voltammetry of TBT thin films on indium tin oxides (ITO). The compound displayed irreversible oxidations under experimental conditions. The oxidation peak maximum of TBT was found at 0.8 V vs Ag/AgCl. The HOMO level of TBT was estimated from the first oxidation onsets to be −5.11 eV, well aligned with the work function of gold (φ = 5.1 eV), and leads to a very low contact resistance between the electrode and organic semiconductor interface.[14]

Figure 1a shows the UV−vis absorption spectrum of thin films of ABT and TBT evaporated under device conditions. The maximum absorption wavelength of TBT thin film locates at 580 nm, as compared with 469 nm for ABT. We can conclude that the absorption wavelength maximum increases by about 111 nm when an additional benzene ring is added to ABT. From the long wavelength absorption edge we calculated the optical band gap of TBT to be 1.97 eV, higher than that of pentacene

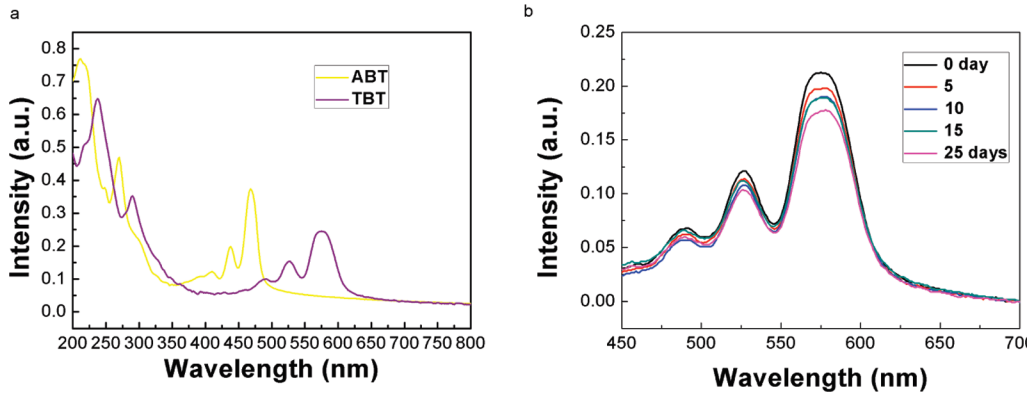

Figure 1. (a) UV−vis spectra of TBT thin film, with that of ABT as comparison, and (b) intensity changes of TBT thin film upon storage at ambient conditions.

TABLE 1: Electrochemical and Photophysical Data of TBT, ABT, and Pentacene

compd	T_{dec}/°C	λ_{max}^{abs}/nm[c]	E_{ox}/V	HOMO[d]/eV	E_g[e]/eV
TBT	339	580	0.8	−5.11	1.97
ABT[a]	300	469	1.15	−5.35	2.5
pentacene[b]	330		0.64	−4.6	1.77

[a] From ref 13. [b] From ref 15a. [c] Absorption maxima of the thin films. [d] Estimated from the onset of oxidation peak (HOMO = $-(4.44 + E_{ox}^{onset})$ eV). [e] Estimated from the onset of absorption peak ($E_g = 1240$ eV λ_{onset}^{-1}).

and similar to that of tetraceno[2,3-*b*]thiophene (TCT).[15] It is worth noting that no significant UV−vis absorption intensity change was observed for TBT thin film after nearly one month under ambient conditions (Figure 1b). And the absorption intensity of pentacene and TCT was reported to decay to zero in 1 h.[15] Such good photostability of TBT should be attributed to the lower HOMO levels, similar to that of PST.[16] Table 1 summarizes the thermal, photophysical, and electrochemical properties of TBT together with ABT and pentacene for comparison.

X-ray Diffraction Characterization. The powder X-ray diffraction pattern of TBT was recorded in transmission mode at ambient temperature (Figure 2a). It has been reported that the crystalline phase of some materials can be obtained from the powder XRD files.[17] From Figure 2a we can conclude that the TBT powder is highly crystalline. With a similar structure, the crystal structure of TBT should be similar to the structure of ABT, with a planar molecule stacking in herringbone geometry similar to pentacene.[13]

Figure 2b shows the XRD profile of TBT thin films at about 60 nm deposited at different substrate temperatures (T_{sub}). The XRD profile of TBT thin films indicates a primary diffraction peak at $2\theta = 5.23°$ with the second-order diffraction peaks at $2\theta = 10.60°$. The same angular position of the reflections indicates that both film and powder exhibit the same crystalline phase. All the films exhibit well-resolved higher order reflections, indicating well-ordered, layered microstructures. Specifically, the film deposited at 40 °C showed similar diffraction peaks up to multiorders with that of 30 °C but higher intensity than that of 30 °C. When a temperature increase to 60 °C, strong peak intensity at $2\theta = 21.2°$ appears with four other diffraction peaks at higher diffraction angles, indicating a higher crystallinity order of the thin films. However, the devices showed decreased mobility at 60 °C, as shown in the following part. Since most of the channel current flows in the first two monolayers of material,[18,19] such mobility-lowering defects might be masked by overgrowths and not be readily visible. The limitation of the diffration method may be responsible for the phenomenon, since most of the X-ray diffraction signal was obtained from the bulk of the sample. And the morphology of the bulk might differ from that of the first two monolayers of materials. From the first diffraction peak at $2\theta = 5.23°$, which is an interlayer peak, we obtained a *d*-spacing of 16.89 Å. As compared with the molecular length of TBT (15.8 Å) based on the extended molecular lengths optimized by ChemDraw 3D and calculated by Material Studio 3.0, we assume that the TBT molecule was standing near upright on the OTS/SiO_2/Si surface and formed a perfectly packed structure. Such orientation is known to be favorable for achieving high mobility since the stacking structure would increase intermolecular π overlap and the stacking direction is also consistent with the direction of current flow.[20]

Device Application. Organic field-effect transistors (OFETs) were fabricated in a top-contact configuration with thin films of TBT deposited onto SiO_2/Si or OTS treated SiO_2/Si as active organic semiconductor layers. The substrate temperature was held at 30, 40, and 60 °C during deposition. All the devices showed typical p-channel transistor characteristics under ambient conditions. As expected, the devices fabricated on OTS treated substrates showed better performance than that of bare SiO_2/Si substrate because of the increased contact angle, enlarged semiconductor grains, and reduced trap density achieved by surface modification.[21] The typical output and transfer characteristics of TBT are shown in Figure 3. The main parameters of device performance, i.e., mobility (μ_{FET}), threshold voltage (V_T), and I_{on}/I_{off} at different substrate temperatures (T_{sub}) are summarized in Table 2. The best device performance with a mobility of 0.13 cm^2 V^{-1} s^{-1} and an on/off ratio of about 7×10^5 was obtained when TBT was deposited on OTS/SiO_2/Si at $T_{sub} = 40$ °C. When deposited at 30 °C, the devices showed mobility of 0.11 cm^2 V^{-1} s^{-1}, similar to that of $T_{sub} = 40$ °C. When substrate temperature increased up to 60 °C, the devices based on TBT exhibited decreased mobility of 0.066 cm^2 V^{-1} s^{-1}. The decrease of device performance may be due to the abnormal crystallization of the thin films at higher substrate temperature, which can be confirmed by X-ray diffraction (XRD) of the thin films. As compared with other acene analogues that showed good performance at high substrate temperature, TBT exhibits a great advantage for use in flexible plastic substrates which cannot withstand high temperatures.

Interestingly, thin film transistors of TBT also show a photoeffect, thus we investigated the photoeffect of TBT devices fabricated on OTS/SiO_2/Si at $T_{sub} = 40$ °C. From Figure 4 we can see that the transfer curves of the device show a large change under white light irradiation with a low power of 30 μWcm^{-2}. The ratio of photocurrent to dark-current (I_{ph}/I_{dark}) with a value higher than 10^4 was obtained at $V_g = 20$ V. This excellent I_{ph}/I_{dark} ratio is larger than that of most reported organic phototransistors[22] and comparable to that of amorphous silicon,[23] suggesting the devices can be well controlled according to the light illumination and the gate voltage. This result further indicated the great potential application of TBT in organic electronics.

Morphology. To better understand the relationship between thin film morphology and mobility, the TBT thin films at different substrate temperatures were investigated by AFM. As we know, the morphological features of thin films depend significantly on the substrate temperatures.[24] From Figure 5 containing the AFM images of TBT thin films on OTS/SiO_2/Si surface at different substrate temperatures, we can see that when the T_{sub} increased from 30 to 40 °C, more uniform substrate coverage and an improvement in film connectivity occurred. The morphology improvement should be responsible for the high mobility of the thin film at $T_{sub} = 40$ °C. When the substrate temperature increases to 60 °C, the grain sizes increase further and the density of the grain boundaries decreases, but the thin film showed lower mobility. We attributed the abnormal mobility change to the abnormal thin film crystallization, as shown in the XRD pattern. Figure 5b shows the AFM images of compound ABT, and the grain sizes of ABT were much larger than that of TBT, inducing higher mobility (maximum 0.41 cm^2 V^{-1} s^{-1} at 20 °C) of ABT devices.

Density Functional Theory Calculations and Structure−Property Relationships. When compared with ABT, TBT showed inferior device performance, although the mobility of TBT is still comparable to that of amorphous silicon. This comparison raises a host of very interesting questions: Does the length of conjugation unit matter? What is the best unit length for acenes and heteroacenes to obtain the best device

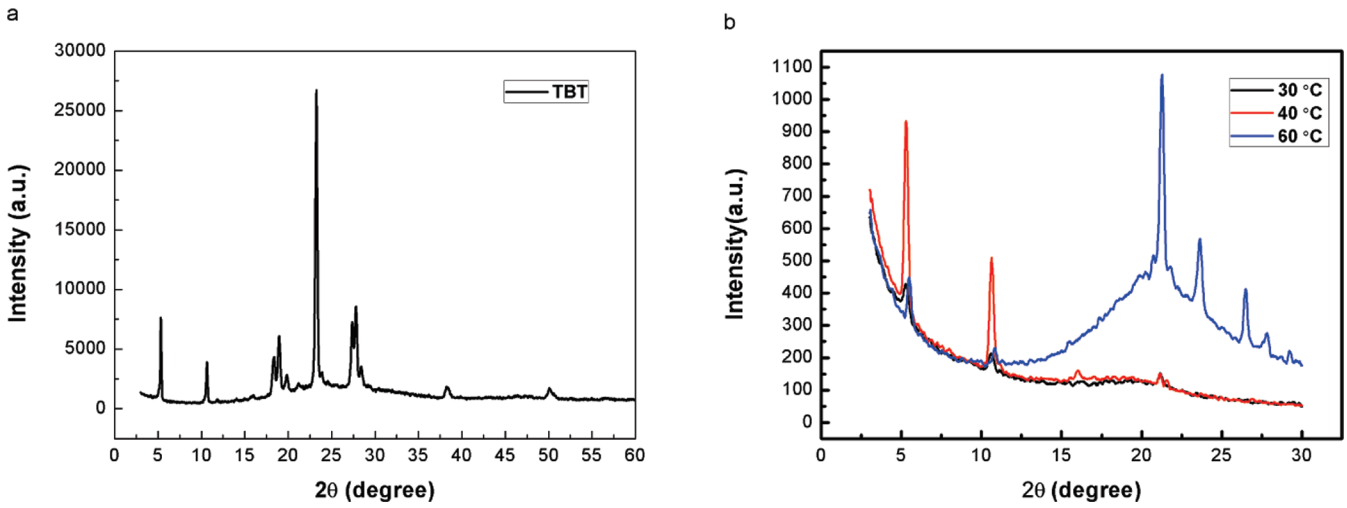

Figure 2. (a) X-ray diffraction patterns of TBT powder. (b) X-ray diffractograms of TBT thin films on OTS treated SiO_2/Si fabricated at T_{sub} = 30, 40, and 60 °C.

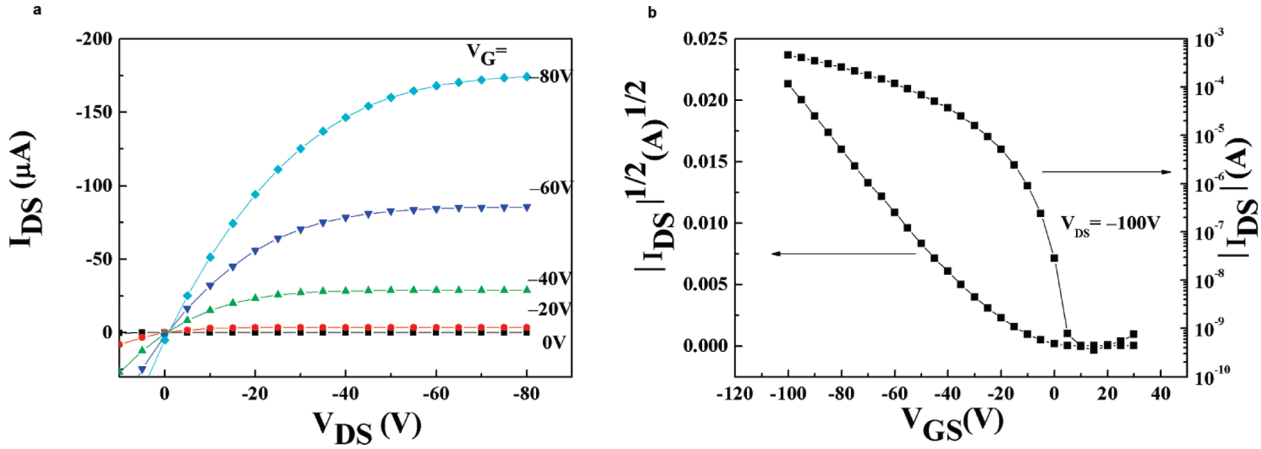

Figure 3. Output (a) and transfer (b) curves of TBT device deposited on OTS treated substrate at 40 °C (channel length 50 μm, channel width 3 mm).

TABLE 2: FET Characteristics of TBT

	bare SiO_2			OTS treated SiO_2		
T_{sub} (°C)	μ	I_{on}/I_{off}	V_{th} (V)	μ	I_{on}/I_{off}	V_{th} (V)
30	0.042	10^5	−25	0.11	5×10^5	−20
40	0.052	3×10^5	−28	0.13	7×10^5	−23
60	0.025	10^5	−23	0.066	2×10^5	−17

performance? To have a better understanding of the relationship between structure and properties of heteroacenes, we performed theoretical calculations at the density functional theory (DFT)/B3LYP/6-31G(D) level on compound TBT using Gaussian 03,[25] with compound ABT for comparison. Accordingly, DFT optimization on TBT leads to practically planar conformations, similar to ABT. We analyzed the frontier orbitals on these conformations. As can be observed in Figure 6, the HOMO level of TBT, found at −4.76 eV, is a combination of tetracene and thiophene π bonding orbitals. At the same time, the HOMO level of ABT, found at −5.05 eV, is a combination of anthracene and thiophene π bonding orbitals, indicating decreased conjugation length by one benzene ring than TBT. The calculated band gap values are 2.52 and 3.16 eV for TBT and ABT, respectively. Bao's group has reported that increasing the conjugation length of linear acenes could increase the mobility.[15b] But our study with TBT showed lower mobility than ABT, contrary to the early report. This distinct phenomenon may be due to the following facts. Specifically, unlike other linear acenes, TBT

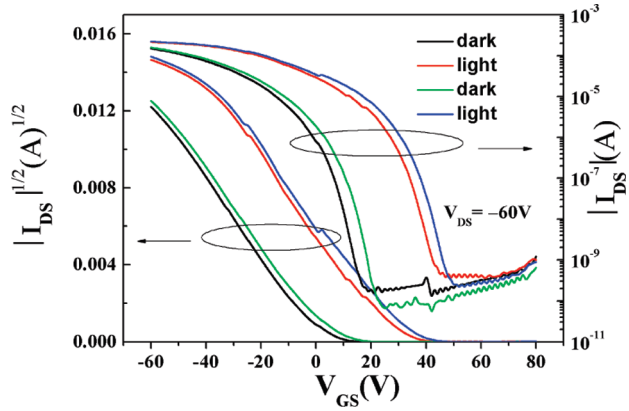

Figure 4. Transfer curves of TBT phototransistor device deposited on OTS treated substrate at 40 °C under dark and light conditions.

and ABT both have a bent backbone in which the end benzene rings in the dibenzothiophene unit deviated much from the main linear conjugation backbone. The higher aspect ratio (the ratio of the length of a molecule to its width)[15b,26] of the bent molecule, like TBT compared to ABT, may lead to weaker intralayers interactions, that is, a lower energy barrier against nucleus formation, both of which increase the rate of nucleation, and result in smaller grain in the thin films. These thin films

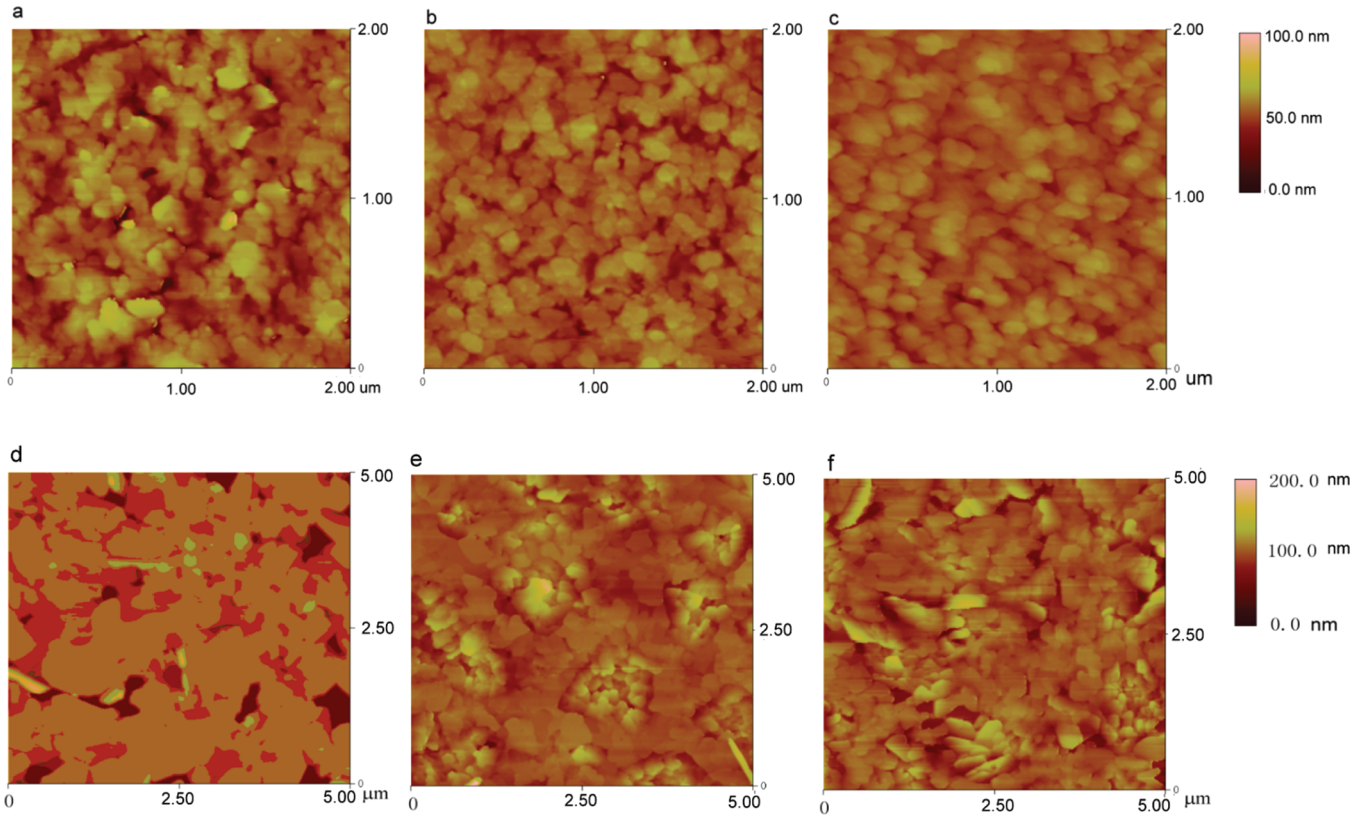

Figure 5. AFM images of TBT thin films deposited on OTS treated substrate at different substrate temperatures (a, 30 °C; b, 40 °C; c, 60 °C) and the AFM images of comparative compound ABT at different temperatures (d, 20 °C; e, 40 °C; f, 60 °C).

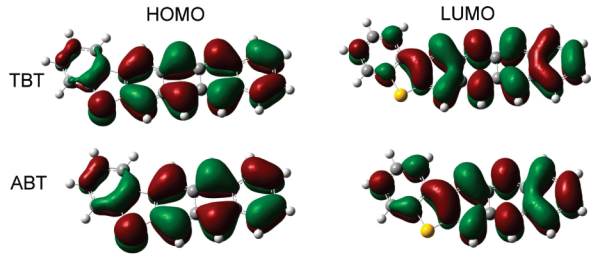

Figure 6. HOMO and LUMO levels for TBT and ABT according to DFT calculations at the B3LYP/6-31G(D) level.

have more grain boundaries and hence a lower mobility, which have been confirmed by the AFM images of TBT and ABT thin films.

Conclusions

In summary, we report here a new hexacene analogy, TBT, prepared by a facile method from commercially available materials in large quantities. The compound showed red-shifted UV−vis absorption peaks as compared with its five-ring analogy ABT, indicating higher conjugation length. FETs and phototransistors were both fabricated with TBT as semiconducting layers. As compared with that of ABT (0.41 $cm^2 V^{-1} s^{-1}$), TBT showed lower mobility (0.13 $cm^2 V^{-1} s^{-1}$). We investigated the phenomenon through XRD, AFM of the thin films, and DFT calculations. Finally we concluded that devices performance of the two compounds is influenced greatly by thin film morphology. Further investigations probing the structure−property relationships of bent heteroacenes are underway.

Experimental Section

Instruments and Measurement. ^{1}H NMR (400 MHz) spectra were obtained on a Bruker DMX-300 NMR spectrometer with tetramethylsilane as internal standard. High-resolution mass spectra (HRMS) and EI MS were both recorded on a Micromass GCT-MS spectrometer. Elemental analyses were performed on a Carlo Erba model 1160 elemental analyzer. Electronic absorption spectra were measured on a Jasco V570 UV−vis spectrophotometer. TGA-DTA measurements were carried out on a TA SDT 2960 instrument under a dry nitrogen flow, heating from room temperature to 500 °C, with a heating rate of 10 deg/min. Cyclic voltammetry measurements were carried out in a conventional three-electrode cell with Pt button working electrodes of 2 mm diameter, a platinum wire counter electrode, and a Ag/AgCl reference electrode on a computer-controlled CHI660C instruments at room temperature. X-ray diffraction (XRD) measurements were carried out in the reflection mode at room temperature, using a 2-kW Rigaku X-ray diffraction system. AFM measurements were carried out with a Nanoscope IIIa instrument (Digital Instruments) operating in tapping mode.

Materials Synthesis. Tetrahydrofuran and dichloromethane were distilled before use. Other Chemicals and solvents were purchased from commercial resources and used without further purification.

***3-(Dibenzothiophene-2-carbonyl)-2-naphthoic Acid* (1).** To a solution of 4 g of aluminum chloride in dichloromethane (100 mL) was added a suspension of 1.98 g (10 mmol) of naphtho[2,3-*c*]furan-1,3-dione in 20 mL of dichloromethane. The resulting yellow suspension was stirred for 30 min and then a solution of dibenzothiophene (2 g, 11 mmol) in 20 mL of dichloromethane was added dropwise under cooling with ice. The reaction mixture was then allowed to stir for 4 h at room temperature, and then was poured into a solution of 100 mL of water and 40 mL of concentrated hydrochloric acid. The layers were separated and the combined organic layers were dried, evaporated under vacuum, and purified by recrystallization from

ethanol to afford 3.2 g (84%) of 3-(dibenzothiophene-2-carbonyl)-2-naphthoic acid as a light pink solid. EI-MS: *m*/*z* 382 (M^+). ^{1}H NMR (400 MHz, $CDCl_3$): δ 7.48−7.56 (m, 2H), 7.71−7.76 (m, 2H), 8.05−8.14 (m, 4H), 8.21−8.23 (m, 1H), 8.34−8.39 (m, 1H), 8.66−8.67 (d, 1H), 13.16 (s, 1H).

3-(Dibenzothiophene-2-ylmethyl)naphthalen-2-yl-methanol (2). To a solution of 1.91 g (5 mmol) of compound **1** in 50 mL of NaOH solution was added 1.58 g (25 mmol) of Zn powder. The suspension was heated to reflux for 24 h then cooled to room temperature. HCl (10%) was added to the mixture until the pH 2. White precipitate was collected by filtration and dried. Then the crude product was dissolved in ether and 0.57 g (15 mmol) of $LiAlH_4$ was added in one portion. The mixture was heated to reflux for 2 h, and then was poured into a solution of 100 mL of water and 40 mL of concentrated hydrochloric acid. The layers were separated and the organic layers were extracted with ether and combined. Final product was obtained by evaporating the solvent under vacuum and purified by column chromatography on silica gel with petroleum ether:ethyl acetate (2:1) as the eluent, affording 1.06 g (60%) of compound **2** as a white solid. EI-MS: *m*/*z* 354 (M^+). ^{1}H NMR (400 MHz, $CDCl_3$): δ 3.92 (s, 2H), 4.90 (s, 2H), 5.39 (bs, 1H), 6.73 (s, 1H), 7.36−7.38 (d, 1H), 7.41−7.52 (m, 2H), 7.54−7.64 (m, 2H), 7.70−7.91 (m, 4H), 8.07−8.12 (m, 2H), 8.58 (s, 1H). Anal. Calcd for $C_{24}H_{18}OS$: C 81.32, H 5.12. Found: C 81.50, H 5.01.

3-(Dibenzothiophene-2-ylmethyl)-2-naphthaldehyde (3). Compound **2** (1.77 g, 5 mmol) was dissolved in 50 mL of CH_2Cl_2, PCC (15 mmol) was added, and the mixture was stirred for 5 h at room temperature. Brown solution was obtained after filtration of the mixture, affording crude product upon evaporation of solvent. Purified compound **3** as a light yellow oil (1.58 g, 90%) was obtained by column chromatography on silica gel with petroleum ether:ethyl acetate (5:1) as the eluent. EI-MS: *m*/*z* 352 (M^+). ^{1}H NMR (400 MHz, $CDCl_3$): δ 4.78 (s, 2H), 7.33−7.35 (d, 1H), 7.41−7.46 (m, 2H), 7.55−7.59 (m, 1H), 7.62−7.66 (t, 1H), 7.69−7.71 (d, 1H), 7.77−7.79 (d, 1H), 7.82−7.85 (t, 2H), 8.00−8.02 (d, 2H), 8.07−8.09 (d, 1H), 8.39 (s, 1H), 10.29 (s, 1H). ^{13}CNMR (100 MHz, D-DMSO): δ 82.95, 120.31, 121.77, 122.03, 122.86, 123.42, 124.56, 125.43, 127.12, 127.16, 127.18, 128.01, 128.31, 129.08, 129.93, 133.31, 133.60, 134.93, 135.98, 136.42, 139.84, 140.45, 143.55, 170.35. Anal. Calcd for $C_{24}H_{16}OS$: C 81.79, H 4.58. Found: C 81.46, H 4.32.

Tetraceno[2,3-b]benzo[d]thiophene (TBT). To 1.4 g (4 mmol) of compound **3** in a 50 mL bottle was added 10 g of PPA, then the mixture was heated to 100 °C for 2 h. After cooling to room temperature, the slurry mixture was poured into cold water and stirred for 1 h. The precipitate was collected and dried to afford crude product TBT, which was recrystallized to give TBT as a deep purple powder. EI-MS: *m*/*z* 334 (M^+). ^{1}H NMR (600 MHz, D-ODCB): δ 5.88 (s, 1H), 6.01 (s, 1H), 7.26−7.33 (m, 3H), 7.34 (m, 1H), 7.46 (s, 1H), 7.51 (s, 1H), 7.65−7.66 (d, 1H), 7.70−7.71 (t, 2H), 7.79 (s, 1H), 7.96−7.99 (t, 2H). Anal. Calcd for $C_{24}H_{14}S$: C 86.19, H 4.22. Found: C 86.20, H 4.24.

Device Fabrication. FETs were fabricated with top contact configuration. A thin film of about 50 nm was vacuum deposited on octadecyltrichlorosilane (OTS) treated Si/SiO_2 substrate at different substrate temperature. An n-type Si wafer with a SiO_2 layer of 500 nm and a capacitance of 7.5 nF cm^{-2} was used as the gate, and gold source and drain contacts (50 nm) were deposited on the organic layer through a shadow mask. The channel length (L) and width (W) were 50 μm and 3 mm, respectively. The FET measurements were carried out at room temperature in air, using a Keithley 42 SCS semiconductor parameter analyzer. The mobility of devices based on ABT was calculated in the saturation regime. The equation was listed as follow:

$$I_{DS} = (W/2L)C_i\mu(V_{GS} - V_T)^2$$

where μ is the field-effect mobility, L and W are the channel length and width, respectively, C_i is the insulator capacitance per unit area, and V_{GS} and V_T are the gate voltage and threshold voltage, respectively.

The phototransistor devices were fabricated in similar manner with the FET devices above-mentioned with $W = 8800$ μm and $L = 80$ μm. Output curves are changed by the light effect (with a power of 30 μW cm^{-2}) with a measurement step of 1 V. One of the important merits of the phototransistor is the ratio of photocurrent and dark-current P, which was calculated with the equation:

$$P = \text{signal/noise} = I_{ph}/I_d = (I_l - I_{dark})/I_{dark}$$

where I_{ph} is the photocurrent, I_l the drain current under illumination, and I_{dark} the drain current in the dark.

Acknowledgment. We acknowledge financial support from the National Natural Science Foundation of China (20825208, 60736004, 20721061), the National Major State Basic Research Development Program (2006CB806203, 2006CB932103, 2009CB623603), and the Chinese Academy of Sciences.

References and Notes

(1) (a) Clar, E. *Polycyclic Hydrocarbons*; Academic Press: London, UK, 1964; Vol. 1, p 4. (b) Anthony, J. E. *Angew. Chem., Int. Ed.* **2008**, *47*, 452. (c) Wu, J.; Pisula, W.; Mullen, K. *Chem. Rev.* **2007**, *107*, 718. (d) Ong, B. S.; Wu, Y.; Li, Y.; Liu, P.; Pan, H. *Chem.—Eur. J.* **2008**, *14*, 4766. (e) Kelley, T. W.; Baude, P. F.; Gerlach, C.; Ender, D. E.; Muyres, D.; Haase, M. A.; Vogel, D. E.; Theiss, S. D. *Chem. Mater.* **2004**, *16*, 4413. (f) Sun, Y.; Liu, Y.; Zhu, D. *J. Mater. Chem.* **2005**, *15*, 53. (g) Di, C.; Yu, G.; Liu, Y.; Zhu, D. *J. Phys. Chem. B* **2007**, *111*, 14083.

(2) (a) Schwab, P. F. H.; Smith, J. R.; Michl, J. *Chem. Rev.* **2005**, *105*, 1197. (b) Melucci, M.; Favaretto, L.; Bettini, C.; Gazzano, M.; Camaioni, N.; Maccagnani, P.; Ostoja, P.; Monari, M.; Barbarella, G. *Chem.—Eur. J.* **2007**, *13*, 10046. (c) Murphy, A. R.; Frechet, J. M. J. *Chem. Rev.* **2007**, *107*, 1066.

(3) (a) Deng, W.-Q.; Goddard, W. A., III *J. Phys. Chem. B* **2004**, *108*, 8614. (b) Wen, S.-H.; Li, A.; Song, J.; Deng, W.-Q.; Han, K.-L.; Goddard, W. A., III *J. Phys. Chem. B* **2009**, *113*, 8813.

(4) (a) Cicoira, F.; Santato, C.; Dinelli, F.; Murgia, M.; Loi, M. A.; Biscarini, F.; Zamboni, R.; Heremans, P.; Muccini, M. *Adv. Funct. Mater.* **2005**, *15*, 375. (b) Gundlach, D. J.; Nichols, J. A.; Zhou, L.; Jackson, T. N. *Appl. Phys. Lett.* **2002**, *80*, 2925. (c) Buurma, A. J. C.; Jurchescu, O. D.; Shokaryev, I.; Baas, J.; Meetsma, A.; de Wijs, G. A.; de Groot, R. A.; Palstra, T. T. M. *J. Phys. Chem. C* **2007**, *111*, 3486. (d) Syed Abthagir, P. S.; Ha, Y.-G.; You, E.-A.; Jeong, S.-H.; Seo, H.-S.; Choi, J.-H. *J. Phys. Chem. B* **2005**, *109*, 23918.

(5) (a) Nelson, S. F.; Lin, Y.-Y.; Gundlach, D. J.; Jackson, T. N. *Appl. Phys. Lett.* **1998**, *72*, 1854. (b) Gundlach, D. J.; Lin, Y.-Y.; Jackson, T. N.; Nelson, S. F.; Schlom, D. G. *IEEE Electron Device Lett.* **1997**, *18*, 87. (c) Klauk, H.; Halik, M.; Zschieschang, U.; Schmid, G.; Radlik, W.; Weber, W. *J. Appl. Phys.* **2002**, *92*, 5259. (d) Klauk, H.; Halik, M.; Zschieschang, U.; Eder, F.; Schmid, G.; Dehm, C. *Appl. Phys. Lett.* **2003**, *82*, 4175. (e) Volkel, A. R.; Street, R. A.; Knipp, D. *Phys. Rev B* **2002**, *66*, 195336. (f) Fritz, S. E.; Kelley, T. W.; Frisbie, C. D. *J. Phys. Chem. B* **2005**, *109*, 10574.

(6) (a) Bendikov, M.; Duong, H. M.; Starkey, K.; Houk, K. N.; Carter, E. A.; Wudl, F. *J. Am. Chem. Soc.* **2004**, *126*, 7416. (b) Bailey, W. J.; Liao, C.-W. *J. Am. Chem. Soc.* **1955**, *77*, 992.

(7) (a) Mondal, R.; Adhikari, R. M.; Shah, B. K.; Neckers, D. C. *Org. Lett.* **2007**, *9*, 2505. (b) Mondal, R.; Shah, B. K.; Neckers, D. C. *J. Am. Chem. Soc.* **2006**, *128*, 9612.

(8) Payne, M. M.; Parkin, S. R.; Anthony, J. E. *J. Am. Chem. Soc.* **2005**, *127*, 8028.

(9) Chun, D.; Cheng, Y.; Wudl, F. *Angew. Chem., Int. Ed.* **2008**, *47*, 8380.

(10) Kaur, I.; Stein, N. N.; Kopreski, P. P.; Miller, G. P. *J. Am. Chem. Soc.* **2009**, *131*, 3424.

(11) Tang, M. L.; Mannsfeld, S. C. B.; Sun, Y.-S.; Becerril, H. A.; Bao, Z. *J. Am. Chem. Soc.* **2009**, *131*, 882.

(12) Okamoto, T.; Kudoh, K.; Wakamiya, A.; Yamaguchi, S. *Chem.—Eur. J.* **2007**, *13*, 548.

(13) (a) Du, C.; Guo, Y.; Liu, Y.; Qiu, W.; Zhang, H.; Gao, X.; Liu, Y.; Qi, T.; Lu, K.; Yu, G. *Chem. Mater.* **2008**, *20*, 4188. (b) Guo, Y.; Du, C.; Di, C.; Zheng, J.; Sun, X.; Wen, Y.; Zhang, L.; Wu, W.; Yu, G.; Liu, Y. *Appl. Phys. Lett.* **2009**, *94*, 143303.

(14) Burgi, L.; Richards, T. J.; Friend, R. H.; Sirringhaus, H. *J. Appl. Phys.* **2003**, *94*, 6129.

(15) (a) Tang, M. L.; Okamoto, T.; Bao, Z. *J. Am. Chem. Soc.* **2006**, *128*, 16002. (b) Tang, M. L.; Reichardt, A. D.; Okamoto, T.; Miyaki, N.; Bao, Z. *Adv. Funct. Mater.* **2008**, *18*, 1579. (c) Valiyev, F.; Hu, W.-S.; Chen, H.-Y.; Kuo, M.-Y.; Chao, I.; Tao, Y.-T. *Chem. Mater.* **2007**, *19*, 3018.

(16) Cicoira, F.; Santato, C.; Dadvand, A.; Harnagea, C.; Pignolet, A.; Bellutti, P.; Xiang, Z.; Rosei, F.; Meng, H.; Perepichka, D. F. *J. Mater. Chem.* **2008**, *18*, 158.

(17) (a) Desiraju, G. R.; Gavezzotti, A. *J. Chem. Soc., Chem. Commun.* **1985**, *41*, 907. (b) Desiraju, G. R.; Gavezzotti, A. *Acta Crystallogr., Sect. B* **1989**, *45*, 473.

(18) Laquindanum, J. G.; Katz, H. E.; Lovinger, A. *J. Am. Chem. Soc.* **1998**, *120*, 664.

(19) Torsi, L.; Dodabalapur, A.; Katz, H. E. *J. Appl. Phys.* **1995**, *78*, 1088.

(20) Delongchamp, D. M.; Sambasivan, S.; Fischer, D. A.; Lin, E. K.; Chang, P.; Murphy, A. R.; Frechet, J. M. J.; Subramanian, V. *Adv. Mater.* **2005**, *17*, 2340.

(21) (a) Shtein, M.; Mapel, J.; Benziger, J. B.; Forrest, S. R. *Appl. Phys. Lett.* **2002**, *81*, 268. (b) Hayakawa, R.; Petit, M.; Chikyow, T.; Wakayama, Y. *Appl. Phys. Lett.* **2008**, *93*, 153301.

(22) (a) Narayan, K. S.; Kumar, N. *Appl. Phys. Lett.* **2001**, *79*, 1891. (b) Saragi, T. P. I.; Pudzich, R.; Fuhrmann, T.; Salbeck, J. *Appl. Phys. Lett.* **2004**, *84*, 2334. (c) Hamilton, M. C.; Martin, S.; Kanicki, J. *IEEE Trans. Electron Devices* **2004**, *51*, 877. (d) Dutta, S.; Narayan, K. S. *Adv. Mater.* **2004**, *16*, 2151. (e) Xu, Y.; Berger, P. R.; Wilson, J. N.; Bunz, U. H. F. *Appl. Phys. Lett.* **2004**, *85*, 4219.

(23) Kaneko, Y.; Koike, N.; Tsutsui, K.; Tsukada, T. *Appl. Phys. Lett.* **1990**, *56*, 650.

(24) (a) Xia, Q.; Burkhardt, M.; Halik, M. *Org. Electrochem.* **2008**, *9*, 1061. (b) McCulloch, I.; Heeney, M.; Chabinyc, M. L.; Delongchamp, D.; Kline, R. J.; Colle, M.; Duffy, W.; Fischer, D.; Gundlach, D.; Hamadani, B.; Hamilton, R.; Richter, L.; Salleo, A.; Shkunov, M.; Sparrowe, D.; Tierney, S.; Zhang, W. *Adv. Mater.* **2009**, *21*, 1091. (c) Yoshihito, Y.; Takimiya, K.; Toyoshima, Y.; Yamashita, K.; Aso, Y.; Otsubo, T. *J. Mater. Chem.* **2004**, *14*, 1367.

(25) Frisch, M. J. *Gaussian 03*, revision C. 02; Gaussian, Inc., Wallingford, CT, 2004.

(26) Gundlach, D. J.; Nichols, J. A.; Zhou, L.; Jackson, T. N. *Appl. Phys. Lett.* **2002**, *80*, 2925.

JP101135E